Reconnection in a rotation-dominated magnetosphere and its relation to Saturn's auroral dynamics

S. W. H. Cowley,[1] S. V. Badman,[1] E. J. Bunce,[1] J. T. Clarke,[2] J.-C. Gérard,[3] D. Grodent,[3] C. M. Jackman,[1] S. E. Milan,[1] and T. K. Yeoman[1]

Received 21 September 2004; revised 16 November 2004; accepted 3 December 2004; published 4 February 2005.

[1] The first extended series of observations of Saturn's auroral emissions, undertaken by the Hubble Space Telescope in January 2004 in conjunction with measurements of the upstream solar wind and interplanetary magnetic field (IMF) by the Cassini spacecraft, have revealed a strong auroral response to the interplanetary medium. Following the arrival of the forward shock of a corotating interaction region compression, bright auroras were first observed to expand significantly poleward in the dawn sector such that the area of the polar cap was much reduced, following which the auroral morphology evolved into a spiral structure around the pole. We propose that these auroral effects are produced by compression-induced reconnection of a significant fraction of the open flux present in Saturn's open tail lobes, as has also been observed to occur at Earth, followed by subcorotation of the newly closed flux tubes in the outer magnetosphere region due to the action of the ionospheric torque. We show that the combined action of reconnection and rotation naturally gives rise to spiral structures on newly opened and newly closed field lines, the latter being in the same sense as observed in the auroral images. The magnetospheric corollary of the dynamic scenario outlined here is that corotating interaction region-induced magnetospheric compressions and tail collapses should be accompanied by hot plasma injection into the outer magnetosphere, first in the midnight and dawn sector, and second at increasing local times via noon and dusk. We discuss how this scenario leads to a strong correlation of auroral and related disturbances at Saturn with the dynamic pressure of the solar wind, rather than to a correlation with the north-south component of the IMF as observed at Earth, even though the underlying physics is similar, related to the transport of magnetic flux to and from the tail in the Dungey cycle.

Citation: Cowley, S. W. H., S. V. Badman, E. J. Bunce, J. T. Clarke, J.-C. Gérard, D. Grodent, C. M. Jackman, S. E. Milan, and T. K. Yeoman (2005), Reconnection in a rotation-dominated magnetosphere and its relation to Saturn's auroral dynamics, *J. Geophys. Res.*, *110*, A02201, doi:10.1029/2004JA010796.

1. Introduction

[2] Although the Saturn flybys by the Pioneer 11 and Voyager 1 and 2 spacecraft in the interval 1979–1981 provided much information about the large-scale structure of the magnetic field and plasma populations in Saturn's magnetosphere [e.g., *Smith et al.*, 1980; *Ness et al.*, 1981, 1982; *Behannon et al.*, 1983; *Sittler et al.*, 1983; *Richardson*, 1986; *Richardson and Sittler*, 1990], relatively little information has been available until recently concerning the dynamics of the magnetosphere and the nature of its interaction with the interplanetary medium. Voyager observations showed that the power of Saturn kilometric radiation (SKR) emission is strongly positively correlated with the dynamic pressure of the solar wind [*Desch*, 1982; *Desch and Rucker*, 1983], though the physical mechanism underlying the correlation has remained unclear. SKR is believed to be generated by the accelerated electron beams associated with Saturn's polar auroras [e.g., *Lecacheux and Genova*, 1983; *Galopeau et al.*, 1995], thus implying a related interplanetary modulation of electron precipitation and auroral emission. A number of individual high-resolution images of Saturn's UV auroras obtained by the Hubble Space Telescope (HST) over past years have indeed shown a highly variable auroral morphology [*Gérard et al.*, 1995, 2004; *Trauger et al.*, 1998; *Cowley et al.*, 2004a], but in the absence of upstream data it has not been possible to relate these to concurrent interplanetary conditions. Recently, however, *Prangé et al.* [2004] have discussed a HST image showing a polar auroral disturbance that they infer was triggered by the passage of an interplanetary shock associated with a coronal mass ejection (CME), tracked from the Sun via Earth and Jupiter.

[3] With the approach of the Cassini spacecraft to Saturn prior to its insertion into orbit on 1 July 2004 the opportu-

[1]Department of Physics and Astronomy, University of Leicester, Leicester, UK.
[2]Center for Space Physics, Department of Astronomy, Boston University, Boston, Massachusetts, USA.
[3]Institut d'Astrophysique et de Géophysique, Université de Liège, Liège, Belgium.

0148-0227/05/2004JA010796

nity was taken during the interval 8–30 January 2004 to obtain a sequence of images of Saturn's auroras using the HST, in conjunction with upstream Cassini measurements of the interplanetary medium and SKR emissions. Initial results have demonstrated that both UV auroras and SKR emissions respond strongly to the shock compressions that are associated with interplanetary corotating interaction regions (CIRs) [*Clarke et al.*, 2005; *Crary et al.*, 2005; *Kurth et al.*, 2005]. In this paper we discuss the implications of these observations and suggest a qualitative interpretive scenario based on reconnection dynamics in a rotation-dominated magnetosphere. This scenario should form the basis of future more quantitative evaluations. We begin in section 2 by providing an overview of the joint Cassini-HST observations which form the basis for the theoretical discussion which follows.

2. Observations of CIR-Related Auroral Activity at Saturn

[4] A summary of the observations to be discussed here is shown in Figure 1. Figures 1a–1d show four HST Space Telescope Imaging Spectrograph UV frames of the auroras in Saturn's southern polar region, which was tilted toward the Sun (and Earth) during the epoch of these observations. The images in Figures 1a–1d were obtained on 24, 26, 28, and 30 January 2004, respectively. These frames have been generated by combining individual images obtained on a given HST orbit in the red-green-blue color system. For each date the frame includes clear images (blue), F25SRF2 filtered images (red), and the mean of all images (green), with a total exposure time of ~50 min (the center times of these intervals are given in Figure 1 caption). This leads to nearly 30° of rotational blurring for any feature that rigidly corotates with the planet but distinguishes auroral emissions from reflected sunlight from the disc and rings by their blue and red colors. Each frame shows a log stretch in intensity, identical for each day, with the upper threshold set to a value ~20 kR to emphasize the faint emissions.

[5] Figure 1e shows the interplanetary magnetic field (IMF) strength observed by Cassini over the relevant interval (24–30 January), together with the estimated reconnection voltage (open flux production rate) at Saturn's dayside magnetopause, derived using the algorithm of *Jackman et al.* [2004]. This voltage is taken to be given by

$$\Phi = V_{SW} B_{\perp} L_o \cos^4(\theta/2), \quad (1)$$

where V_{SW} is the radial speed of the solar wind, $B_{\perp}$ is the strength of the IMF component perpendicular to the radial flow, L_o is a scale length taken equal to 10 Saturn radii (R_S = 60330 km) by analogy with Earth, and θ is the clock angle of the IMF relative to Saturn's northern magnetic axis. Details of the plasma and field measurements employed are given by *Crary et al.* [2005], while the reader is referred to *Jackman et al.* [2004] for further discussion of the origins of the formula. According to equation (1), large dayside reconnection voltages are favored for northward pointing IMF at Saturn, opposite to the case for Earth due to the opposite sense of the planetary field. During the interval shown in Figure 1 the spacecraft was located ~0.2 AU upstream of Saturn in the radial direction and was also displaced from the planet-Sun line by ~0.5 AU toward dawn. With a nominal solar wind speed of ~500 km s^{-1} the radial propagation delay from the spacecraft to the planet was thus ~17 hours. Using this nominal delay, the timing of the HST images relative to the interplanetary data is shown in Figure 1e by the vertical dashed lines. We note, however, that the relative timing is unavoidably uncertain to within several hours, due particularly to nonradial propagation effects and the separation of the spacecraft and planet in heliographic longitude [*Crary et al.*, 2005].

[6] The sizable displacement between the spacecraft and planet during the interval also means that the plasma and field properties measured by Cassini may not be indicative in detail of those that impinged on the planet, but they should certainly be representative of the overall properties and behavior. In particular, heliosphere-scale structures such as CIRs which are observed by Cassini will certainly impinge on the planet with an appropriate (but somewhat uncertain) delay. CIR structures are formed by the interactions of solar wind plasmas of differing speed that are emitted by the rotating Sun into a given radial direction, with slow wind originating from the region surrounding the solar magnetic dipole equator and fast wind from the coronal holes surrounding the magnetic poles [e.g., *Gosling and Pizzo*, 1999]. Fast wind following slow into a given direction forms a compression region, while slow wind following fast forms a rarefaction. The interval considered here corresponds to the declining phase of the solar cycle, during which the effective solar magnetic dipole had a significant tilt with respect to the solar spin axis. This configuration leads to a consistent structure in the near-equatorial heliosphere consisting of two compression regions per solar rotation, separated by two rarefactions. This recurrent CIR pattern sweeps around with the rotating Sun over both spacecraft and planet and was observed by Cassini over many solar rotations surrounding the interval of interest here [*Jackman et al.*, 2004].

[7] The field data in Figure 1 show that at the beginning of the interval the IMF strength was relatively low at a few tenths of a nanotesla, as had continuously been the case for several days previously, corresponding to a CIR rarefaction region. The estimated dayside reconnection voltages are therefore also low, varying from small values to peaks of several tens of kilovolts. The HST image obtained at the end of 24 January (Figure 1a) relates to these conditions and shows a "quiet" but relatively expanded auroral oval that had also remained of similar form for several days previously [*Clarke et al.*, 2005]. The previous CIR compression had been observed by Cassini during the interval 15–17 January, following which the auroral oval had increased modestly in size to that seen in Figure 1a. A sudden increase in field strength then occurred at the spacecraft at ~1600 UT on 25 January, indicative of the arrival of the forward shock of a CIR compression region (indicated by the vertical arrow marked "S" in the figure). Simple radial modeling indicates that the shock arrived at Saturn at ~0800 UT on 26 January after a delay of ~16 hours [*Crary et al.*, 2005], a timing which does not differ significantly from the nominal ~17 hours used here in Figure 1. It is thus estimated that the shock arrived ~30 hours after Figure 1a and ~10 hours prior to Figure 1b, which was obtained at ~1900 UT on 26 January. Figure 1b shows that major auroral dynamics

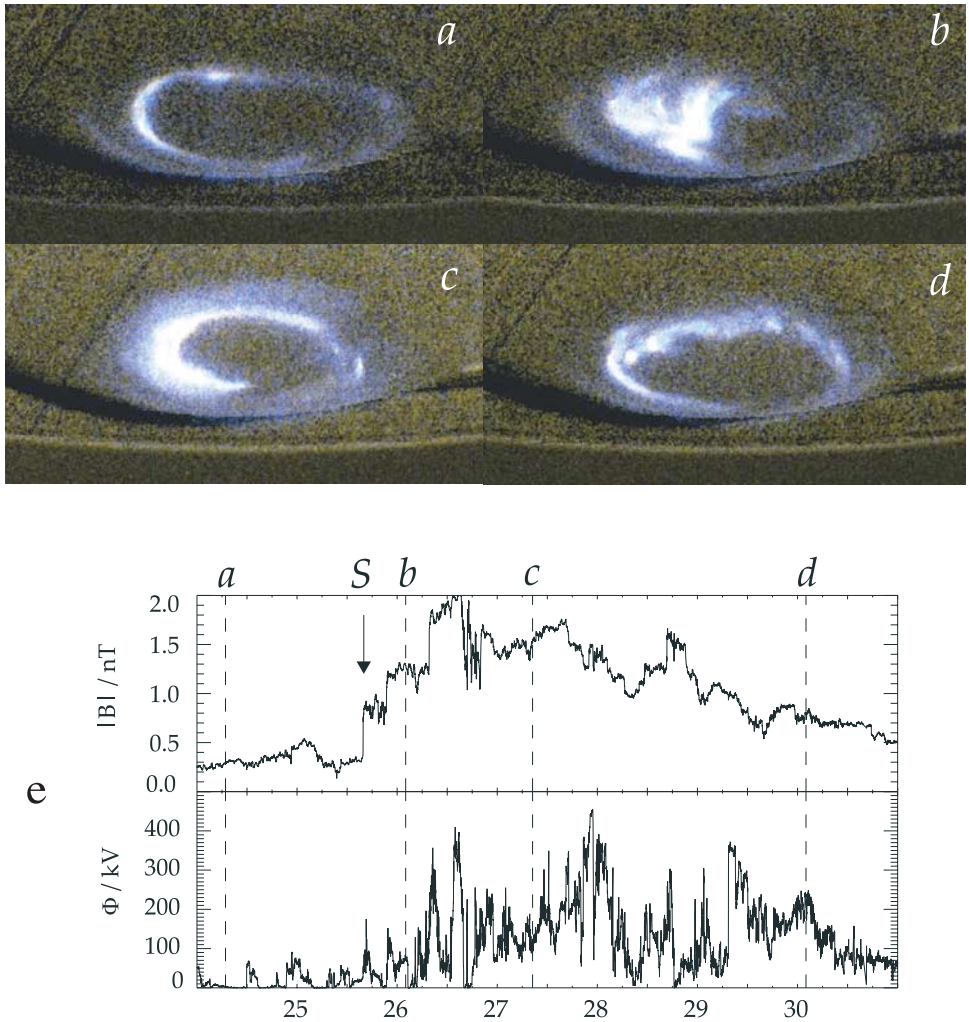

Figure 1. Overview of Saturn's auroral dynamics and their relation to CIR compression regions as observed during the Cassini-HST campaign in January 2004. At the top of the figure we show four frames of Saturn's UV auroras in the southern polar region obtained by the HST as follows: (a) 2351 UT on 24 January, (b) 1903 UT on 26 January, (c) 0128 UT on 28 January, and (d) 1902 UT on 30 January. Clear and filtered images from a given HST orbit have been combined in the red-green-blue color system as indicated in section 1, the total integration time in each frame being ~50 min. Times given are the approximate midtimes of the imaging intervals involved. Noon-midnight meridian is near the center of each frame with noon toward the top, dawn to the left, and dusk to the right. (e) Strength of the IMF measured upstream of Saturn by the Cassini spacecraft and an estimate of the dayside reconnection voltage (open flux production rate) obtained from equation (1) [after *Jackman et al.*, 2004]. Interval shown is 24–30 January inclusive. Vertical dashed lines marked a–d indicate the approximate corresponding times of the auroral images using a nominal 17 hour lag between Cassini and Saturn, though these timings are uncertain to within several hours due to possible nonradial propagation effects in the solar wind and the separation of the spacecraft and the planet in heliographic longitude. Vertical arrow marked "S" indicates the arrival of the forward shock of a CIR compression region at the spacecraft, at ~1600 UT on 25 January. HST images are after *Clarke et al.* [2005], and the interplanetary data are from *Crary et al.* [2005].

were then in progress, with the dawn sector of the oval essentially filled with bright UV emissions. SKR emissions show a corresponding enhancement [*Kurth et al.*, 2005], which was observed at Cassini beginning at ~1200 UT on 26 January (W. S. Kurth, personal communication, 2004), an interval of ~7 hours prior to the corresponding HST image. After the passage of the shock the IMF strength at the spacecraft increased stepwise over the next day, peaking at ~2 nT, before falling more gradually over the next ~5 days. The solar wind density behaved correspondingly, while the wind speed varied modestly between ~550 and ~600 km s^{-1} [*Crary et al.*, 2005]. The estimated dayside reconnection voltage in Figure 1 shows behavior related principally to the IMF strength, though also characteristically strongly modulated on shorter, few-hour timescales by variations in the field direction, between small values when the field pointed south to peaks of ~400 kV when it pointed north [*Jackman et al.*, 2004]. The HST image obtained at

~0100 UT on 28 January (Figure 1c) then corresponds to an interval ~40 hours after the arrival of the shock, some hours after the peak fields had arrived at the planet, during an interval of ~100–200 kV estimated dayside driving. It shows a pronounced "spiral" auroral pattern, with strongest emissions in the dawn sector [*Clarke et al.*, 2005]. The central "polar cap" region of low emission had regained an approximately circular shape but was considerably contracted in size relative to Figure 1a. Figure 1d, obtained at ~1900 UT on 30 January, corresponds to an interval late in the declining phase of the event ~110 hours (~4.5 days) after the arrival of the shock, as the field strengths and dayside voltages approached initial values. Here the near-continuous auroral oval had essentially reformed with a central dark polar region expanded compared with Figure 1c, though still somewhat smaller than in Figure 1a, and with considerable brightness variations particularly in the dawn sector. With regard to relationships with other observations, we note that spiral auroral forms akin to that seen in Figure 1c but of lesser intensity have been reported in earlier HST images by *Gérard et al.* [2004] and are also observed in a number of other images obtained during the January HST campaign [*Clarke et al.*, 2005]. Auroral spirals, winding consistently with increasing local time to lower latitudes, thus appear to be a common morphology at Saturn. We also note that the "disturbed" HST image presented by *Prangé et al.* [2004] appears to have some affinities with Figure 1b, though the area of the prenoon polar auroral enhancement is much more fully developed in the case shown here.

[8] It seems reasonable to propose that the auroral variations observed in Figure 1 are those which relate to the SKR-dynamic pressure correlation found previously by *Desch* [1982] and *Desch and Rucker* [1983] using Voyager data, thus providing clues to the origin of this primary interplanetary-modulation effect of Saturn's magnetosphere. Here we suggest that these effects are connected with reconnection dynamics in a rotating magnetosphere, as we now go on to discuss.

3. Reconnection Dynamics in a Rotating Magnetosphere: Paradigm Cases

3.1. Steady Balanced Reconnection

[9] The starting point for this discussion is the steady state picture of the large-scale field and flow in Saturn's coupled magnetosphere-ionosphere system presented by *Cowley et al.* [2004a], illustrated here in Figures 2a–2b. Figure 2a shows the flow in the magnetospheric equatorial plane, extending to the magnetopause, at ~20 R_S in the subsolar region (bottom of the diagram). Three basic regions are shown. In the inner region the plasma rotates in the same sense as the planet, with an angular velocity that falls from near-rigid corotation in the inner region (~10.6 hour period) to ~50–60% of rigid corotation in the outer part of the middle magnetosphere, as indicated by Voyager observations [*Richardson*, 1986, 1995]. The subcorotation of the plasma is believed to be due to particle pickup from internal sources, combined with radial transport [*Saur et al.*, 2004]. Surrounding this is a layer where the planetary plasma is lost down the dusk flank of the tail by plasmoid formation and field line pinch-off, as first discussed in the Jovian context by *Vasyliunas* [1983] (the "Vasyliunas cycle"). The Vasyliunas cycle reconnection line is shown by the dashed line marked with crosses, while the dot-dashed line marked "P" and the dashed streamline marked "O" show the locations of the outer boundary of the plasmoid and its central *O* line, respectively. On the dawn side of the outer magnetosphere we then have the sunward directed "return" flows of closed flux tubes from the tail associated with the reconnection interaction with the interplanetary medium, first discussed in the terrestrial context by *Dungey* [1961] (the "Dungey cycle"). These flows are initiated by open flux production at the dayside magnetopause, quantified by equation (1), following which the open field lines are stretched downstream by the solar wind flow to form the tail lobes, from which flux eventually returns by reconnection closure and sunward flow as depicted in Figure 2a. The corresponding reconnection regions on the magnetopause and in the tail are shown in the figure by the solid lines marked with crosses. The plasma flows in the outer dayside region correspond to angular velocities which are ~50–80% of rigid corotation [*Richardson*, 1986, 1995].

[10] Figure 2b then shows the corresponding flows and field-aligned currents in the polar ionosphere, looking down onto the northern pole with the direction of Sun again at the bottom of the diagram. Upward and downward directed currents are shown by the circled dots and crosses, respectively. The outer boundary of the diagram corresponds to a colatitude of ~30°, mapping to ~3 R_S in the equatorial plane, while the region of open flux, which could not be depicted equatorially in Figure 2a, occupies the central region, to ~15° colatitude. The amount of open flux contained within this region is ~30–40 GWb. The flows within this region consist of the sum of an antisunward flow associated with Dungey cycle transport in the tail lobes combined with subcorotation with the planet driven by ion-neutral collisions in the ionosphere, which twists the tail lobes [*Isbell et al.*, 1984]. Recent infrared Doppler observations obtained by *Stallard et al.* [2004] suggest angular velocities of ~30% of rigid corotation in this region, such that the corresponding flows, of ~800 m s^{-1} at the polar cap boundary, are usually considerably in excess of the ~20–200 m s^{-1} flows associated with the Dungey cycle [*Jackman et al.*, 2004]. The sudden increase in flow speed across the open-closed field line boundary from ~30% of rigid corotation on open field lines to ~50–80% of rigid corotation on outer closed field lines (as indicated above), implies a sudden reduction in the equatorward directed ionospheric Pedersen current, and hence an upward directed field-aligned current at the boundary, indicated in Figure 2b by circled dots. *Cowley et al.* [2004a] showed that for plausible parameters these currents require the downward acceleration of magnetospheric electrons into the ionosphere, thus producing a ring of "discrete" UV emission around the boundary, which they suggested corresponds to the main auroral oval (e.g., Figure 1a). A simplified (axisymmetric) quantitative model has been presented by *Cowley et al.* [2004b]. When the Dungey cycle is active, however, the associated flows enhance the boundary currents and hence auroras at dawn relative to dusk. In addition to these discrete auroras associated with field-aligned currents at the open-closed field line boundary, "diffuse" emissions produced by hot plasma precipitation from the outer magnetosphere may be expected to extend equator-

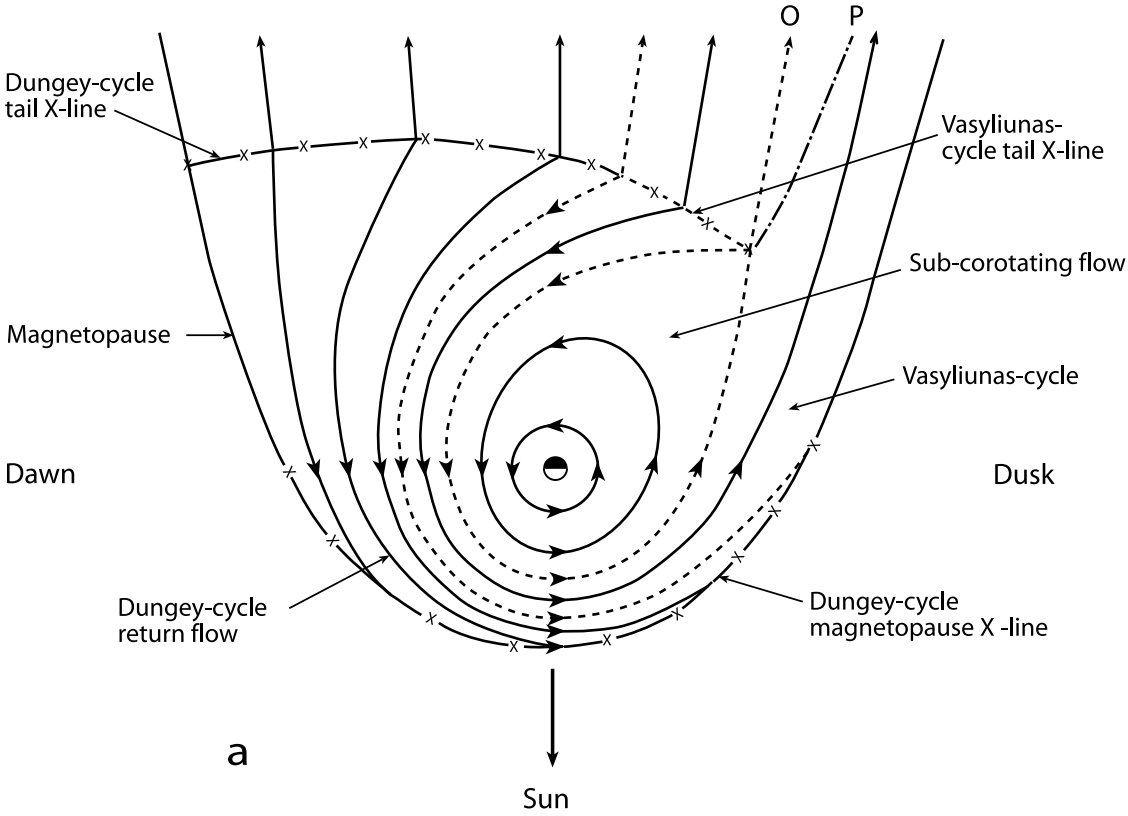

Figure 2a. Sketch of the plasma flow in the equatorial plane of Saturn's magnetosphere out to the magnetopause (at a subsolar distance of $\sim$20 R_S), where the direction to the Sun is at the bottom of the diagram, dusk is to the right, and dawn is to the left. Arrowed solid lines show plasma streamlines, arrowed dashed lines show the boundaries between flow regimes (also streamlines), the solid lines joined by crosses show the reconnection lines associated with the Dungey cycle, and the dashed lines with crosses show the tail reconnection line associated with the Vasyliunas cycle. Line indicated by the O marks the path of the plasmoid *O* line in the Vasyliunas cycle flow (also a streamline), while P marks the outer limit of the plasmoid field lines, which eventually asymptote to the dusk tail magnetopause. (From *Cowley et al.* [2004a].)

ward of the boundary at all local times (see, e.g., section 3.2). In particular, we may expect precipitation from the hot plasmas formed in the nightside reconnection processes associated with the Dungey and Vasyliunas cycles, which should occur downstream from their respective mapped reconnection lines ("*X* lines" in Figures 2a–2b). According to Figure 2b this precipitation should therefore also favor the dawn side of the polar ionosphere. In particular, precipitation of hot plasma resulting from tail reconnection in the Dungey cycle should occur on a layer of streamlines passing from the mapped tail to the mapped magnetopause reconnection regions via dawn as shown. In this steady state picture, therefore, both discrete and diffuse emissions should be enhanced at dawn compared with dusk when the Dungey cycle is active.

3.2. Reconnection Pulses

[11] The situation depicted in Figures 2a–2b relates to an interval of steady significant magnetospheric driving by the Dungey cycle, involving equal rates of open flux production at the dayside magnetopause and destruction in the tail. However, it is clear from the results presented by *Jackman et al.* [2004] and those shown in Figure 1 that the magnetopause rate is characteristically variable on both long timescales (days) due to field strength variations in CIR structures and on shorter timescales (tens of minutes to hours) due to north-south field fluctuations. In addition, the auroral data in Figure 1 suggest the occurrence of intervals of impulsive flux closure in the tail, associated with sudden contractions of the polar cap, as will be discussed further in section 4. Here, therefore, we broaden the above considerations to include discussion of the effect of variable reconnection rates at the magnetopause and in the tail, and of intervals of unbalanced dayside and nightside reconnection. Here we begin by consideration of the consequences of brief pulses of reconnection, lasting for intervals much shorter than the planetary rotation period. This topic has been discussed previously in the terrestrial context by *Cowley and Lockwood* [1992] and is now applied here to Saturn. For the case of the Earth the effects of planetary rotation were ignored in the discussion, since corotational effects are expected to be small outside of the small central "core" of dipolar flux tubes corresponding to the plasmasphere. As we have seen above, however, plasma rotation with the planet, driven by ion-neutral coupling in the ionosphere, is a major feature at Saturn, both on closed

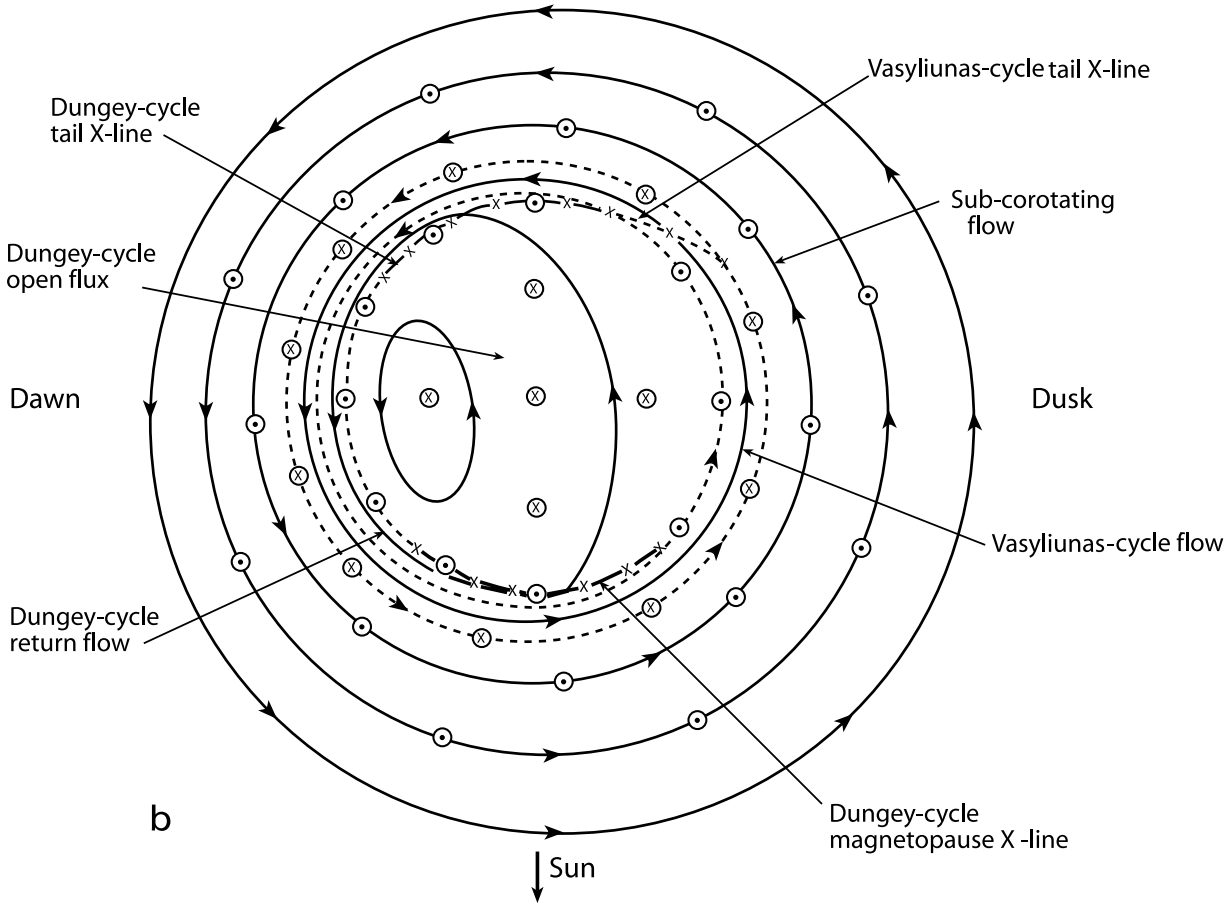

Figure 2b. Sketch of the plasma flow in Saturn's northern ionosphere in a format following that of Figure 2a, where the direction to the Sun is at the bottom of the diagram, dusk is to the right, and dawn is to the left. Outermost circle corresponds to a colatitude of $\sim 30^\circ$ from the pole, which maps magnetically in the equatorial plane to a radial distance of $\sim 3\ R_S$. Circled dots and crosses indicate regions of upward and downward field-aligned current, respectively, as indicated by the divergence of the horizontal ionospheric current. Pedersen currents flow generally equatorward and close in the field-aligned current system shown, while Hall currents flow generally anticlockwise around the pole and close in the ionosphere. (From *Cowley et al.* [2004a].)

and open field lines. Here we therefore consider the transport and assimilation of newly reconnected field lines in the presence of such rotational flows.

[12] We begin in Figure 3 by considering the motion of a small region of newly closed field lines created by a burst of reconnection in the tail. The diagrams show a cut through the equatorial plane as in Figure 2a, where the outer solid line is the magnetopause, and the solid line across the nightside tail represents schematically the outer limit of closed field lines. Plasma streamlines are indicated by the dashed lines with arrows. In Figure 3a a short burst of tail reconnection has closed a small region of open flux in the tail, causing the nightside boundary of closed field lines to bulge outwards. The newly closed flux is indicated in Figure 3 by the stippling, with an inner boundary indicated by the short-dashed line. It is shown to be located on the dawn side of the tail due to the possible presence of Vasyliunas cycle outflow at dusk, as in Figure 2a, though for simplicity the latter has not been represented here. We comment on this further below. Initially the field line tension in the newly closed flux tubes causes them to contract toward the planet, while the ionospheric torque imparts a rotation toward dawn. Simple estimates based on the analyses of *Vasyliunas* [1994] and *Cowley and Bunce* [2003] suggest that plausible timescales for the impartation of planetary rotation are ~ 1 hour. After a few hours, therefore, the region of newly closed flux rotates into the dawn boundary of the tail, where it may cause the magnetopause to bulge outwards, as shown in Figure 3b. Solar wind compression resists this outward motion, however, and enforces assimilation of the newly closed flux tubes into the outer region of subcorotating magnetospheric flow. The tubes thus continue to rotate around in the outer magnetosphere as shown in Figures 3c and 3d, where the difference in flux tube cross section depicted reflects schematically the difference in equatorial field strength between the dayside and nightside outer magnetospheres due to the solar wind flow asymmetry. The overall transport time for a full rotation from Figure 3a to Figure 3d is rather uncertain, with plasma angular velocities which are likely to be higher on the dayside than on the nightside. However, the observations cited in section 3.1 suggest that an overall figure of

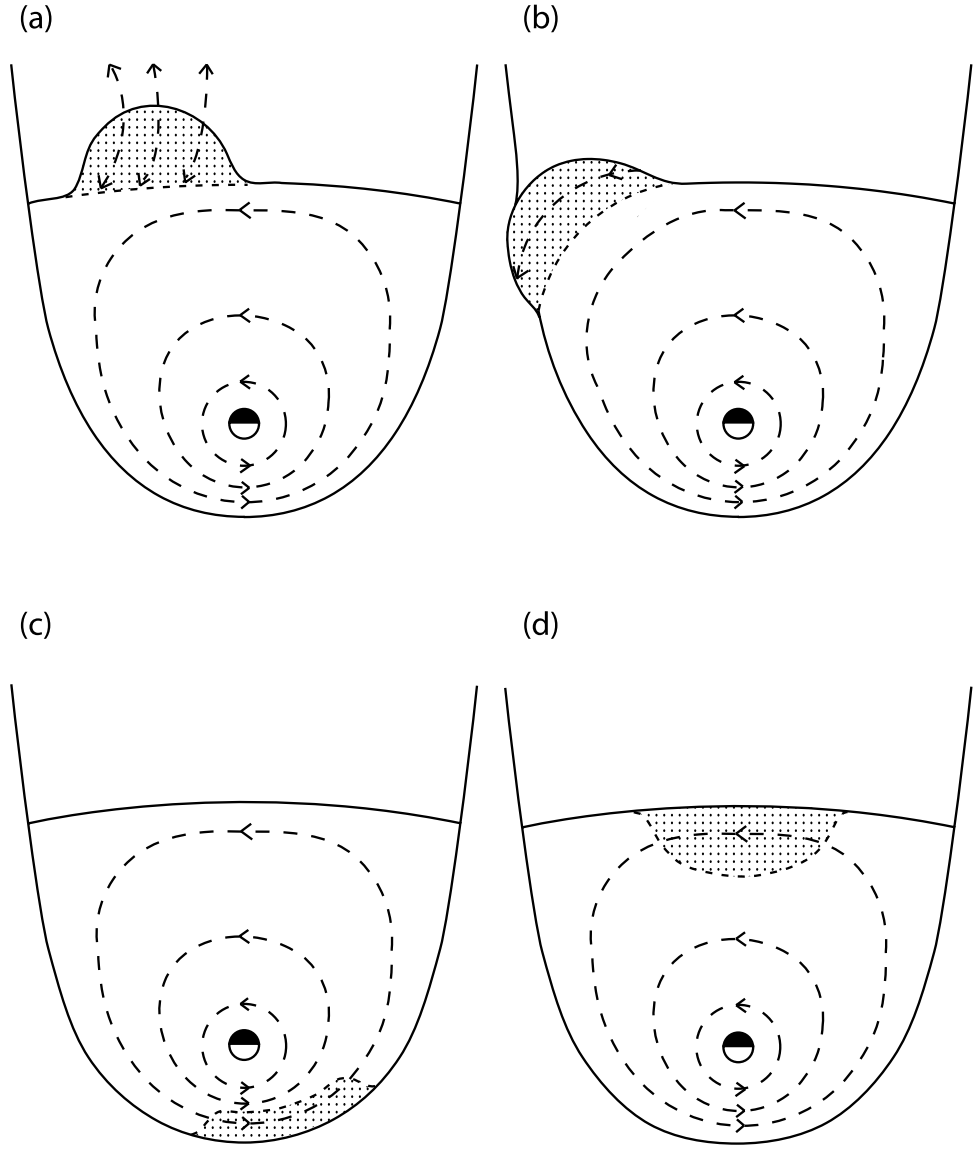

Figure 3. (a–d) Sketches in the equatorial plane showing the motion of a patch of newly closed field lines formed by a burst of reconnection in Saturn's tail. Outer solid line is the magnetopause with the direction to the Sun at the bottom of the diagram, dawn is to the left, and dusk is to the right, as in Figure 2a. Solid horizontal line across the tail shows schematically the outer limit of closed field lines. Streamlines are shown by the dashed lines with arrows. Patch of newly closed flux is indicated by the stippled area, bounded on its inner side by the short-dashed line.

~50% of rigid corotation may not be unreasonable, such that the timescale depicted from Figure 3a to Figure 3d is roughly 20 hours. Ultimately, of course, the patch of new closed flux loses its specific identity, becoming part of the outer magnetosphere region of closed field lines carrying hot plasma from the tail (together possibly with outwardly diffused cool planetary plasma after some time), all of which have similar histories.

[13] In Figure 4 we show the corresponding patterns of flow and precipitation in the northern ionosphere, in a similar format to Figure 2b. In Figure 4a the newly reconnected flux tubes form a "bulge" of closed flux protruding into the polar cap region of open field lines (again shown stippled), on which we expect hot plasma to precipitate following heating in the reconnection process in the tail. Such bulges may occur preferentially on the dawn side of midnight as shown due to the presence of Vasyliunas cycle outflow at dusk, though for simplicity the latter is again not specifically represented here. The hot plasma precipitation may enhance the ionospheric conductivity within the bulge, leading to enhanced boundary currents and auroras as indicated. The ionospheric flow is not strongly perturbed, however, since at this very early stage the field line motions in the tail are largely inductive and do not map directly to the ionosphere. In Figure 4b the assimilation process is in progress, resulting in the elimination of the bulge and a return to a more circular boundary shape, but with a smaller radius than before the reconnection burst. The assimilation is associated with the excitation of a twin-vortex flow, added to the rotational flow as shown,

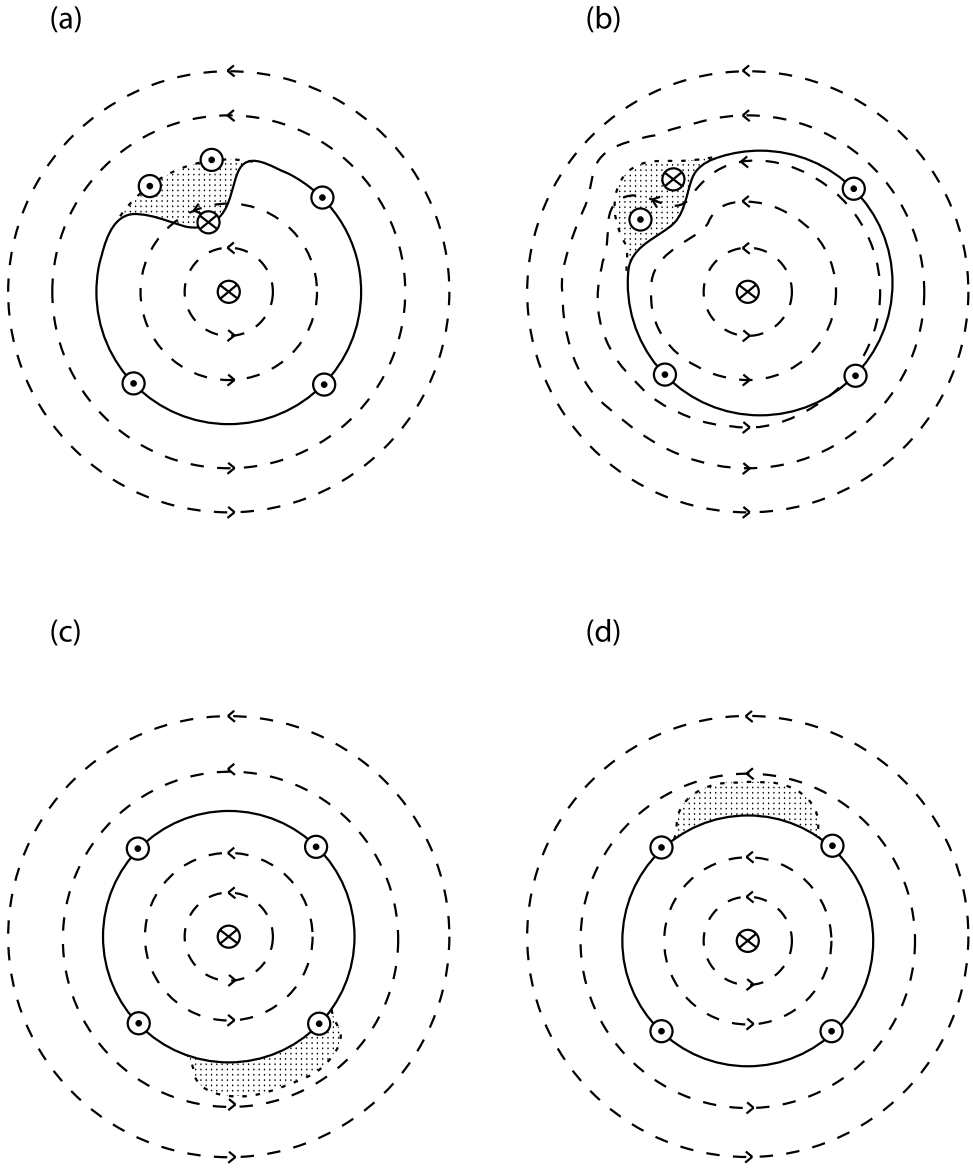

Figure 4. (a–d) Sketches in the ionosphere corresponding to Figure 3, showing the motion of a patch of newly closed field lines formed by a burst of reconnection in the tail. Direction toward the Sun is at the bottom of each diagram, with dawn to the left and dusk to the right, as in Figure 2b. As in Figure 3, the solid line shows the boundary between open and closed field lines, while the dashed lines with arrows show plasma streamlines. Patch of newly closed flux is again indicated by the stippled area, bounded on its equatorward side by the short-dashed line. Circled dots and crosses indicate regions of upward and downward field-aligned currents, respectively.

in which the plasma motion at the open-closed field line boundary is directed equatorward in the vicinity of the bulge and poleward elsewhere, associated with the contraction of the boundary. In the absence of continuing reconnection, as assumed here, these boundary motions are adiaroic; that is, the boundary moves exactly with the convecting plasma. The twin-vortex flow is also associated with a ''substorm wedge-like'' current system (though of opposite polarity to the case of the Earth due to the opposite planetary field polarity), in which upward and downward field-aligned currents flow in the two vortices at either end of the bulge, being closed in the ionosphere via eastward directed Pedersen currents within the bulge. The upward current region is likely to be associated with enhanced electron precipitation and consequent auroral emission akin to the ''westward traveling surge'' at Earth, though here it is located at the eastern end of the auroral bulge. After assimilation into the closed flux region has taken place, the new patch of closed flux continues to rotate around the boundary as shown in Figures 4c and 4d, while precipitation of hot plasma into the ionosphere declines toward the background level of diffuse precipitation from the outer magnetosphere. The auroral emissions resulting from this precipitation will be located immediately equatorward of the ring of discrete auroras produced by upward directed field-aligned currents at the open-closed field line boundary, as

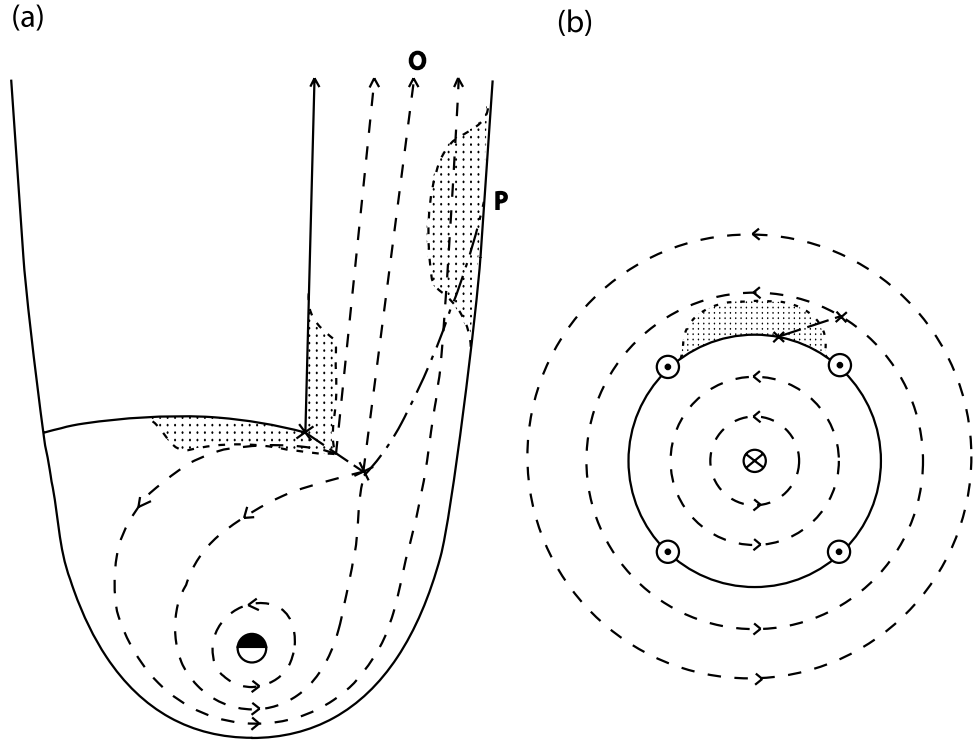

Figure 5. Sketches in the same format as Figures 3 and 4 showing the propagation of a patch of closed field lines into the nightside magnetosphere when the Vasyliunas cycle is active, in the (a) equatorial plane and (b) ionosphere. These diagrams then replace those shown in Figures 3d and 4d, respectively. Labeling of the features of the Vasyliunas cycle field and flow follows that shown in Figures 2a–2b.

described in section 3.1, and will give rise to subcorotating patches of diffuse emission in this region.

[14] The above discussion assumed for simplicity that the region of newly closed flux is assimilated directly into the outer magnetosphere and subsequently subcorotates continuously in this region. If the Vasyliunas cycle is active, however, as depicted in Figures 2a–2b, then these flux tubes will not rotate directly into the nightside closed field region as shown in Figures 3d and 4d, but will instead stretch out along the dusk flank of the tail, overlying other outflowing flux tubes mass-loaded with planetary plasma, before plasmoid formation and pinch-off. The effect of this is indicated in Figure 5a, where we show conditions in the equatorial plane (corresponding to Figure 3d), while in Figure 5b we show conditions in the ionosphere (corresponding to Figure 4d). In the equatorial cut the stippled "newly closed" tubes are flowing down the dusk flank of the magnetopause, and at the instant shown, straddle the dot-dashed line marked P, representing the outer edge of the closed-loop plasmoid. As in Figures 2a–2b, the *O* line of the plasmoid is indicated by the streamline marked O, and the plasmoid inner edge is the solid line streamline emerging from the dawnward end of Vasyliunas cycle *X* line, again indicated by the dashed line marked with crosses. The newly closed field lines at the dusk tail magnetopause which pass through the equatorial plane upstream of the plasmoid outer boundary *P* have not yet taken part in Vasyliunas cycle reconnection and are still connected to the planet's ionosphere, overlying the developing plasmoid structure. Those which pass through the equator downstream of this line have so been reconnected and lie within the plasmoid. They are magnetically connected to the stippled patch of flux lying tailward of the Vasyliunas cycle reconnection line, on the dawnward side of the plasmoid *O* line. On the planetary side of the *X* line the shortened remnants of these field lines (also stippled) emerge into the nightside flow and rotate around with the planet in a similar manner to that shown in Figure 3d. The situation in the ionosphere, shown in Figure 5b, differs little from Figure 4d. The main distinction is that precipitation from the region of newly closed flux may diminish significantly on the upstream side (duskward) of the mapped Vasyliunas cycle reconnection line as the flux tube is stretched out along the dusk tail flank and may then intensify on the downstream (dawnward) side due to the heating of tail plasma in the Vasyliunas cycle reconnection process. The flux tubes may thus brighten aurorally on passing across the mapped *X* line.

[15] We now turn to consider reconnection at the magnetopause, and in Figure 6 we show the corresponding situation in the ionosphere for a pulse of dayside reconnection, in the same format as Figure 4. In Figure 6a the reconnected field lines form a region of newly opened flux, shown stippled, appended to the preexisting region of open flux in the noon sector. These field lines are carried by the combined action of magnetic field tension and magnetosheath flow into the nightside magnetosphere on a timescale of ~2 hours and start to become assimilated into the tail lobe. Precipitation of magnetosheath "cusp" plasma into the ionosphere occurs on these field lines for a similar time, until switched off by the supersonic downstream flow of the magnetosheath source plasma. A twin-vortex flow is again excited in the ionosphere as assimilation takes place, as

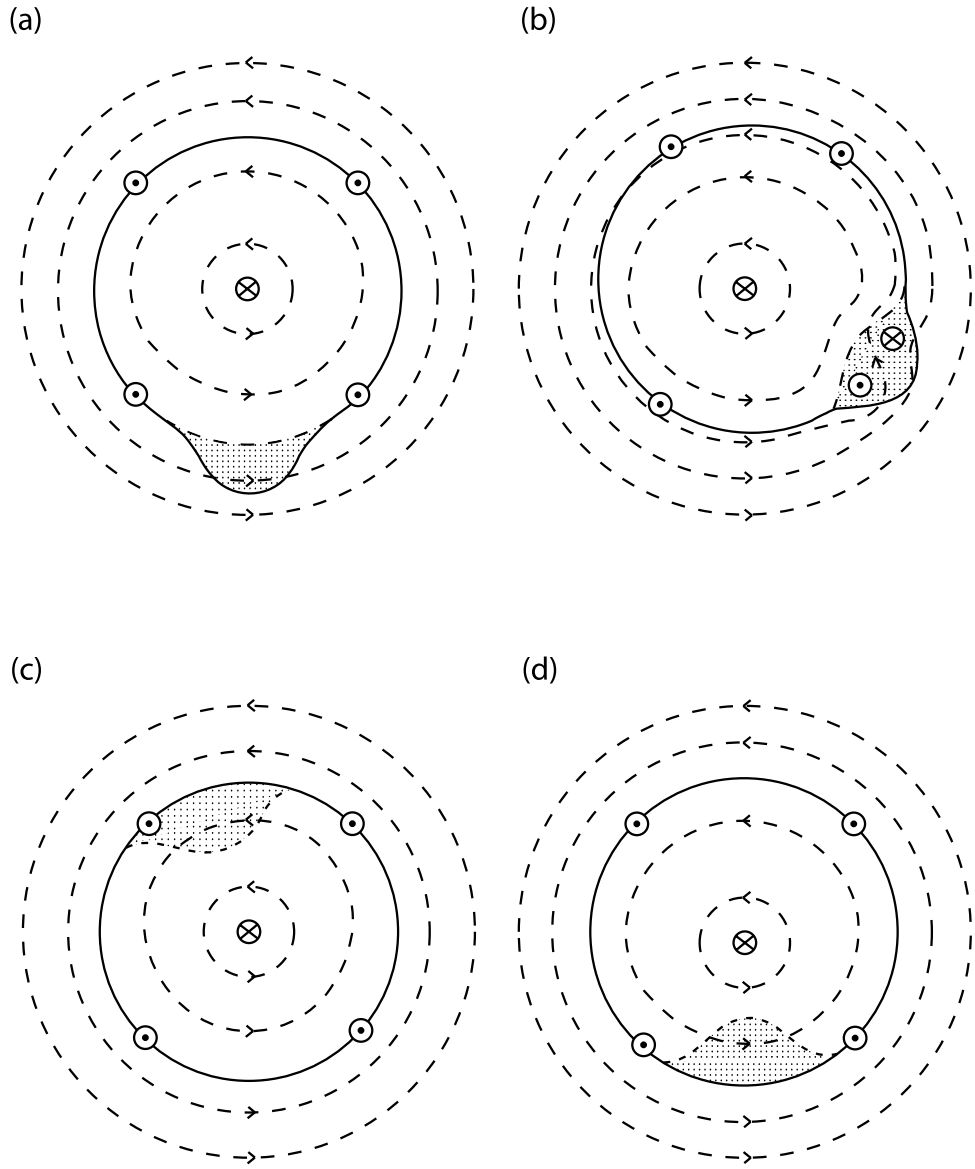

Figure 6. (a–d) Sketches in the ionosphere showing the motion of a patch of newly opened field lines formed by a burst of reconnection at the dayside magnetopause. Format is the same as Figure 4, with the direction toward the Sun at the bottom of each diagram, with dawn to the left and dusk to the right.

shown in Figure 6b, which is such that the perturbed open-closed field line boundary moves poleward in the region of the bulge, and equatorward elsewhere, thus returning the boundary to a more circular shape with the increased amount of open flux. The associated "wedge" current system is again of opposite polarity to that in the terrestrial system. At the same time, ion-neutral frictional drag causes the open tubes to subcorotate around the boundary with the rest of the open field lines, as also shown in Figure 6b. With increasing time, the patch of newly reconnected flux thus simply rotates within the outer part of the region of open flux, as shown in Figures 6c and 6d. This motion causes the open field lines to be twisted into a spiral in the tail lobe as the magnetopause "end" is transported antisunward by the solar wind flow [*Isbell et al.*, 1984]. The down-tail pitch of the spiral (i.e., the down-tail length of one full turn), is thus given by the distance traveled by the solar wind in the time taken for the open field lines to make one complete rotation in the ionosphere. As indicated in section 3.1, the results of *Stallard et al.* [2004] indicate angular velocities of about a third of rigid corotation for this motion, such that the overall timescale for one complete rotation, as shown in Figure 6, is ~30 hours, an interval which we note is much shorter than the typical ~8 day transpolar transit time in the Dungey cycle [*Jackman et al.*, 2004]. With a nominal solar wind speed of ~500 km s^{-1}, the down-tail pitch of the corresponding field spiral in the lobe is thus ~900 R_S. One implication of the spiral structure of the lobe field is that reconnection events occurring in the center of the tail where the two lobes meet will map magnetically in the ionosphere to later local times. For example, a reconnection event occurring in the tail on the midnight meridian at a radial distance of ~225 R_S (one quarter of the above spiral pitch) will map to the ionosphere at dawn. Here, however,

we will assume that tail reconnection events typically occur rather closer to the planet than this, as seems plausible by analogy with Earth. In this case the local time displacements between the tail center and ionosphere will be modest, as effectively assumed in the discussion of Figure 4.

[16] The rotational motion of the open flux has interesting consequences for the structure and dynamics of the tail. In the nonrotating case discussed in the terrestrial context by *Cowley et al.* [1991], sequential pulses of dayside reconnection cause the open flux to become layered in time sequence inside the open-closed field line boundary. Reconnection events on the nightside then cause the open flux to be removed essentially in the same order. In a rotating tail, however, nightside reconnection events will preferentially remove open field lines from the outer part of the open flux region irrespective of when they were opened, and generally these will correspond to relatively recently opened flux tubes which have moved into the nightside with the rotational flow. The consequences of this behavior for the structure and dynamics of Saturn's tail have recently been discussed in detail by *Milan et al.* [2005]. While open field lines at the rim of the polar cap may have relatively short lifetimes, those within the central polar cap may remain open for a much longer interval, thus forming a long tail in the downstream solar wind, until they are closed by a major tail reconnection event which reaches into the center of the tail lobe. Related dynamics apply, of course, to the region of closed field lines as well. That is, the closed magnetic flux which is opened on the dayside by magnetopause reconnection and removed to the tail will generally correspond to flux closed relatively recently within the tail, transported to the dayside by rotation in the outer magnetosphere. The bulk of the subcorotating closed flux within the middle and inner magnetosphere does not take part in this convection cycle.

3.3. Steady Unbalanced Reconnection

[17] A second instructive paradigm case is that of steady unbalanced reconnection. That is, we consider intervals during which the magnetopause and tail reconnection rates are steady, but not the same as each other, such that the amount of open flux in the system changes steadily with time. In Figure 7 we show the situation for a modest level of steady reconnection in the tail, starting at some particular time, but where concurrent magnetopause reconnection is absent. Figures 7a and 7b show the situation in the equatorial plane, where the nightside reconnection region is indicated by the long-dashed lines terminated by the crosses. As in Figure 3, we again assume a preference for the dawn sector due to the possible presence of Vasyliunas cycle outflow at dusk, though for simplicity this is again not represented in Figure 7. Figure 7a shows the situation when the closed field lines formed during the interval (shown stippled) have rotated into the noon sector, while in Figure 7b they have rotated further, back into the postmidnight sector. Assuming an overall rotational angular velocity of around half of rigid corotation in the outer magnetosphere, as indicated in sections 3.1 and 3.2, these diagrams then correspond to times of ~10 and ~20 hours after the tail reconnection started, respectively. We again note that if Vasyliunas cycle outflow is present, the newly closed flux tubes will not rotate back into the midnight sector in the simple manner shown in Figure 7b but will instead stretch out along the dusk flank of the tail with the Vasyliunas cycle flow before pinch-off and plasmoid formation occur, as discussed in section 3.2 in relation to Figure 5. In either case the overall effect of the interval of reconnection is that the region of closed flux in the outer magnetosphere will expand with time, with the most recently reconnected flux at any local time being found in the outermost layer.

[18] Figures 7c and 7d show the corresponding situation in the ionosphere. As in Figure 4, the open-closed field line boundary is shown by the solid line, except in the postmidnight sector where the mapped reconnection region (the "merging gap") is indicated by dashed lines and crosses, where it bulges modestly into the region of open flux. This boundary contracts slowly poleward at all local times as the amount of open flux decreases. The plasma flow at the boundary is directed equatorward across the boundary within the merging gap as open field lines become closed, while elsewhere the contracting boundary moves poleward with the flow. The overall pattern of flow perturbation is thus again of twin-vortex form, added to the rotational flow as shown, and associated with a wedge current system whose field-aligned currents are again shown in the region downstream of the merging gap. Hot plasma formed in the tail reconnection process precipitates into this region forming an auroral bulge. Downstream of the bulge, hot plasma will continue to precipitate on the newly closed field lines, forming an auroral "tail" which extends continuously from the bulge around the boundary via dawn to noon in Figure 7c (after ~10 hours) and then via dusk into the nightside sector in Figure 7d (after ~20 hours). This precipitation will occur immediately equatorward of the discrete auroras associated with the upward field-aligned currents circling the boundary, and it represents a significant enhancement of the general diffuse emissions from the outer magnetosphere. Overall, it can be seen that an interval of unbalanced tail reconnection will produce a spiral pattern of closed field lines and associated precipitation equatorward of the open-closed field line boundary, in which the latitude decreases with increasing local time around the boundary. We note that this is the sense in which the observed spirals are uniquely found to wind in Saturn auroral images [*Gérard et al.*, 2004; *Clarke et al.*, 2005]. Eventually, of course, the individual turns of the spiral lose their specific identities, overall resulting in the formation of an expanded region of hot plasma (and possibly outwardly diffused cool planetary plasma) in the outer magnetosphere.

[19] In Figure 8 we show the corresponding situation in the ionosphere for an interval of magnetopause reconnection in the absence of tail reconnection, in the same format as Figure 7. In this case the open-closed field line boundary expands equatorward at all local times, and the perturbation flow is such that the plasma moves poleward across the boundary in the region of the dayside merging gap as closed flux tubes are opened, while moving equatorward with the expanding boundary at other local times. In Figure 8a the new open flux has rotated from noon to midnight via dusk ~15 hours after the onset of magnetopause reconnection (should the interval last that long), while in Figure 8b a complete ring of "new" open flux has formed around the

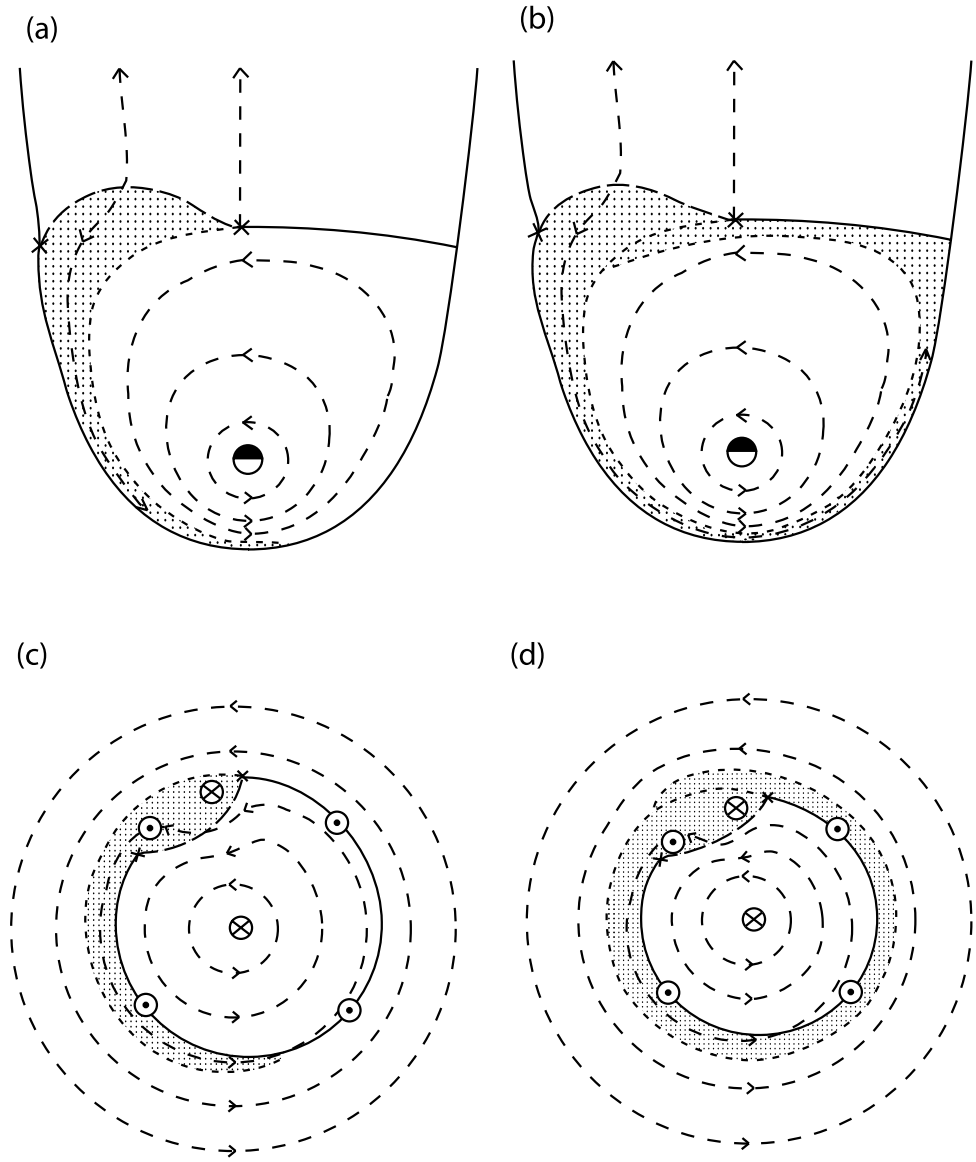

Figure 7. Sketches illustrating the consequences of an interval of modest steady tail reconnection, in the absence of magnetopause reconnection. Shown are conditions in the equatorial plane after (a) ~10 and (b) ~20 hours and (c and d) corresponding conditions in the ionosphere. Format of the figures is the same as Figures 3–6, except that the active reconnection region in the tail, and its mapped counterpart in the ionosphere, is shown by the long-dashed lines terminated with crosses.

boundary after ~30 hours. As time goes on, the new open flux region will thus again form a spiral pattern but now on open field lines associated with polar cap expansion. The sense of the spiral is consequently opposite to that shown in Figure 7, with latitude increasing with increasing local time. We would comment, however, that this scenario is probably rather unrealistic under usual conditions, because dayside reconnection is usually strongly modulated on shorter timescales than those mentioned above due to fluctuations in the IMF direction [*Jackman et al.*, 2004], a point reiterated here in the results shown in Figure 1. In this case the width of the spiral of newly opened field lines will be correspondingly strongly modulated, with a "wide" region being created when the reconnection rate is high during intervals of northward IMF, and a "narrow" region when the reconnection rate is low during intervals of southward IMF. After their creation these wide and narrow bands then subcorotate around in the polar cap until the open field lines are removed by tail reconnection. Our picture is sufficient to emphasize, however, that during intervals when dayside reconnection is effective, the polar cap will be inflated by new open flux addition preferentially into the postnoon and dusk sector, where the boundary is the first to be displaced equatorward. With regard to related auroral features (in addition to the usual discrete and diffuse emissions at and equatorward of the boundary) we would expect these to be confined to the merging gap region near noon, associated with cusp precipitation and the wedge current system present there. As shown in Figure 8, the latter currents enhance the boundary currents on the prenoon side of the

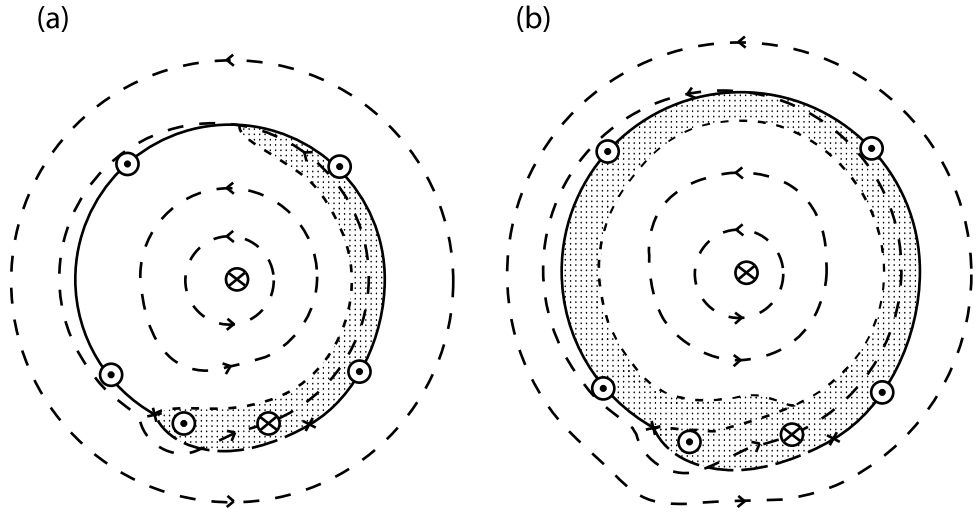

Figure 8. (a and b) Sketches illustrating the ionospheric consequences of an interval of steady magnetopause reconnection in the absence of tail reconnection. Format is the same as in Figures 7c and 7d.

cusp and reduce or reverse the currents on the postnoon side. A detailed discussion of the latter currents and related precipitation has recently been presented by E. J. Bunce et al. (Interplanetary magnetic field control of Saturn's polar cusp aurora, submitted to *Annales Geophysicae*, 2004, hereinafter referred to as Bunce et al., submitted manuscript, 2004). We again note that cusp precipitation should continue only for a few hours downstream of the merging site on a given open field line, as it propagates over the dayside magnetopause following reconnection. Given the timescale of plasma rotation in the open field region (~30 hours), we thus expect cusp precipitation to occur on the newly opened field lines only in the region immediately downstream of the dayside reconnection site.

[20] The conditions discussed above of steady tail reconnection in the absence of magnetopause reconnection, and vice versa, clearly represent limiting cases. In general, reconnection may be active in both regions, but at differing rates with respect to each other. The ionospheric configurations representing these more general conditions are illustrated in Figure 9. In Figure 9a we show the situation in which the tail reconnection rate is higher than the dayside rate, such that overall the region of open flux is contracting with time. In this case the auroral spiral expected to be formed by hot plasma precipitation from newly closed flux tubes flowing around the open-closed field line boundary should still be present (in addition to emissions associated with the field-aligned current systems and diffuse outer magnetosphere precipitation), but its width will be reduced on the dusk side of the mapped magnetopause reconnection region compared with the dawn side. This occurs because the outermost layer of closed tubes now flows to the dayside

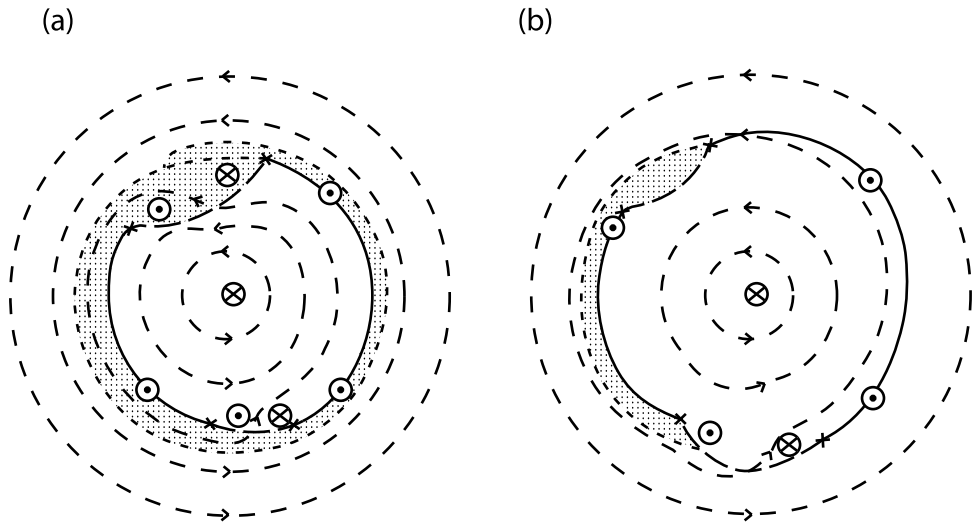

Figure 9. Sketches illustrating the ionospheric consequences of intervals of steady magnetopause and tail reconnection, but where the rates are not equal to each other. (a) Tail reconnection rate exceeding the dayside rate and (b) dayside rate exceeding the tail rate. Format follows that of Figures 4–8.

magnetopause and becomes opened once more, such that the hot plasma escapes into the magnetosheath rather than rotating in the outer magnetosphere past noon to dusk and beyond. In the case shown in Figure 9b where magnetopause reconnection exceeds tail reconnection, however, such that the open flux region expands with time, all of the closed flux reconnected on the nightside flows directly into magnetopause and is opened, such that the region of precipitation of hot plasma is confined to the dawn sector, and a spiral is not formed on closed field lines. However, the usual discrete and diffuse emission will still be present at all local times around the boundary, in addition to features associated with the dayside cusp. We comment again, however, that under usual circumstances, dayside reconnection will be sporadic on timescales of tens of minutes to a few hours, as indicated by *Jackman et al.* [2004] and Figure 1. In this case the situation may therefore typically fluctuate on relatively short timescales between the two situations shown in Figure 9, resulting in the general formation of an auroral spiral but with patchy regions of outer magnetosphere precipitation on the dusk side of noon, as well, of course, as variable precipitation and currents in the dayside cusp.

4. Auroral Response to CIR Compressions

[21] With the above paradigm cases as background, we now return to our discussion of the auroral responses to the CIR compression event summarized in Figure 1. It can be seen from Figure 1 that the central dark polar cap region observed in Figure 1a before the compression had become filled with bright auroras in the dawn sector ~10 hours after the onset of compression in Figure 1b, while after ~40 hours in Figure 1c the auroras formed a bright spiral with a central roughly circular dark region which was considerably contracted compared with Figure 1a. In terms of the discussion in sections 3.2 and 3.3, the poleward expansion of the auroras in Figure 1b, and the contracted polar cap observed in Figure 1c, both strongly suggest a connection with tail reconnection and the closure of open flux in the tail lobes. Following the brief discussion given by *Jackman et al.* [2004], we thus propose that the magnetospheric compression triggered an interval of rapid reconnection in the tail which closed a substantial fraction of the preexisting open flux within a ~10 hour interval and that the HST observed the auroral consequences. Such episodes of rapid closure of major amounts of open lobe flux triggered by interplanetary shocks have occasionally been reported at Earth [e.g., *Petrinec and Russell*, 1996; *Sigwarth et al.*, 2000; *Chua et al.*, 2001; *Boudouridis et al.*, 2003, 2004; *Milan et al.*, 2004; *Meurant et al.*, 2004]. The detailed physical mechanism is as yet unclear, but such magnetospheric compressions will clearly lead to the rapid enhancement of current densities within the plasma sheet and hence to possible instability leading to reconnection. For reasons discussed further in section 5, we here propose that such compression-induced events occur commonly at Saturn in response to CIRs, leading also to the SKR correlation found earlier by *Desch* [1982] and *Desch and Rucker* [1983]. A similar auroral contraction occurred earlier in the Cassini-HST campaign in response to another CIR compression region but was less well observed in HST data than that displayed here in Figure 1 [*Clarke et al.*, 2005; *Crary et al.*, 2005]. We can roughly estimate the tail reconnection rate involved in the event shown in Figure 1 from the auroral images. Assuming that the "dark" central polar region bounded by auroras represents the region of open flux mapping to the tail lobes, the contraction of this region between Figures 1a and 1b implies that roughly ~20 GWb of open flux was closed in the interval between the two images. Assuming further that this occurred wholly during the ~10 hour interval following the arrival of the CIR forward shock prior to Figure 1b, we thus estimate an averaged reconnection rate of ~500 kV over the interval (1 Wb s^{-1} of open flux closure corresponds to a tail reconnection rate of 1 V from Faraday's law). We have no direct means of knowing when the tail reconnection took place during the interval, of course, so that the reconnection rate could have been higher over a proportionately shorter interval. In any event the value is considerably in excess of the estimated dayside reconnection rates during the same interval, of typically several tens of kilovolts as seen in Figure 1, so that during this initial interval, at least, dayside reconnection may be neglected.

[22] Our interpretation of the initial auroral behavior is shown in Figure 10. We suppose that in response to the forward shock of the CIR and subsequent magnetospheric compression an interval of rapid reconnection was initiated in Saturn's magnetic tail in which a significant fraction of the open flux in the lobe was closed over an interval of several hours (a timescale less than Saturn's rotation period). We note from Figure 1a that at the time of the compression the auroral oval was relatively expanded, indicative of a relatively inflated tail system. The equatorial and ionospheric consequences a few hours after the onset of the event (say, 2–3 hours) are illustrated in Figures 10a and 10b, in which new closed flux containing hot plasma on the nightside forms a substantial bulge protruding into the polar cap. This is again shown to occur preferentially on the dawn side of midnight on the assumption that Vasyliunas cycle flow may be active at dusk, as shown, though it seems possible that the distended closed flux tubes in the dusk tail may themselves become pinched off by the compression, with Dungey cycle reconnection then occurring across the whole tail. We also note that if the reconnection region extends quite far down the tail (a significant fraction of the ~900 R_S pitch of the spiral lobe field lines), then the mapping to the ionosphere will also be deflected toward dawn, as discussed in section 3.2. The newly closed flux tubes flow toward the planet in the tail and also rotate into the dawn sector due to the ionospheric torque, possibly forming a bulge on the dawn magnetopause as shown in Figure 10a. In the ionosphere in Figure 10b the auroras will be dominated by the bulge protruding into the postmidnight dark polar region, indicative of the closure of a significant fraction of the open flux in the system, though the usual discrete and diffuse emission will continue to be present at other local times. The perturbed flow in the ionosphere carries the bulge equatorward and toward dawn, acting to distribute the newly closed flux around the boundary and return the region of open flux to a more centered circular shape.

[23] In Figures 10c and 10d we show the situation after ~10 hours, where we suppose that tail reconnection is still

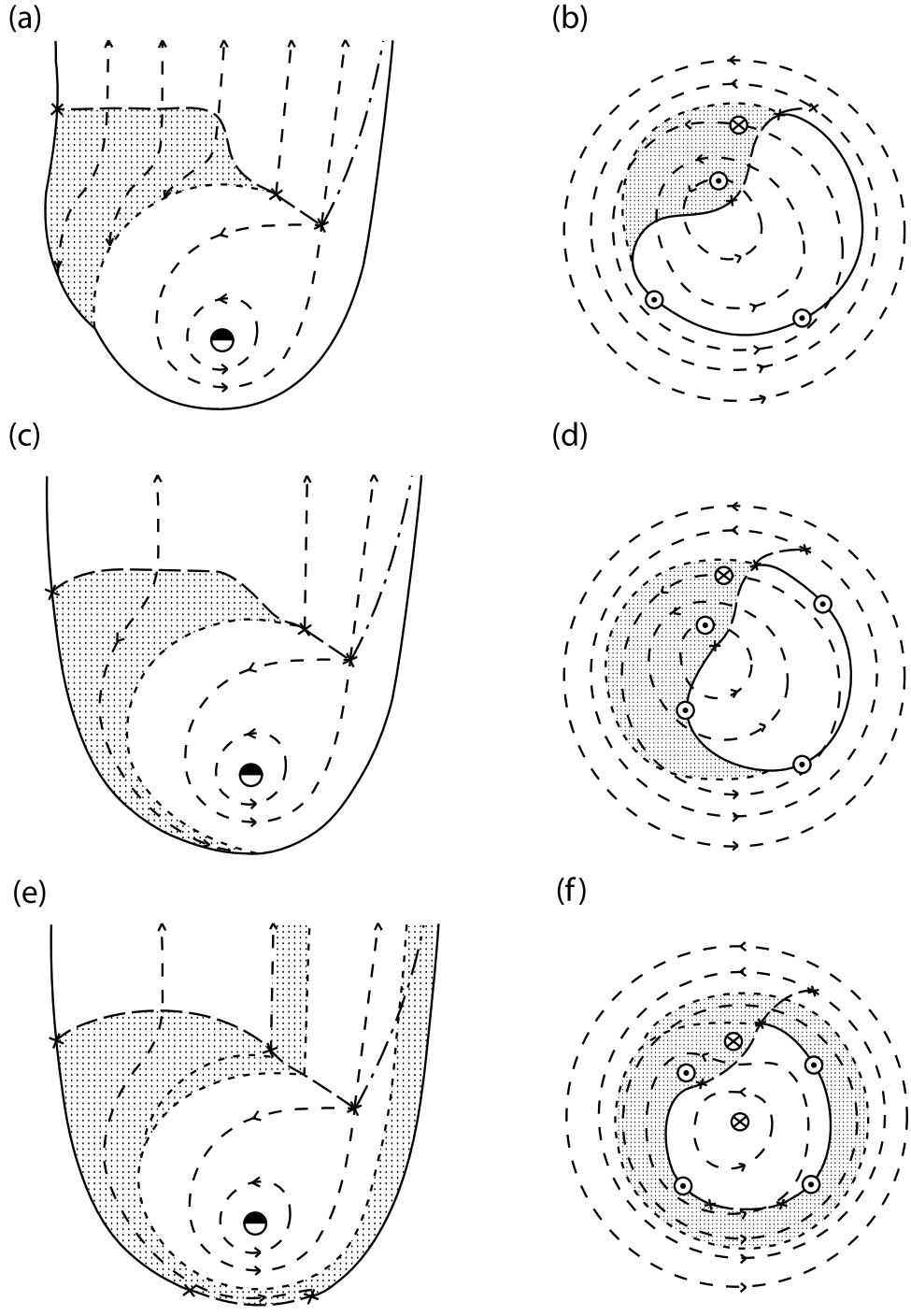

Figure 10. Sketches illustrating the consequences of an interval of rapid reconnection in the tail, in which a significant fraction of the open flux in the tail lobes is closed on a timescale that is short compared with the typical period of plasma subcorotation in the outer magnetosphere (~20 hours). Shown are conditions in the equatorial plane after (a) 2–3, (c) ~10, and (e) ~20 hours and (b, d, and f) corresponding conditions in the ionosphere. Format of the figures is the same as Figures 3–9. In Figures 10e and 10f, dayside reconnection is also in progress.

active but at a declining rate. Overall, we suppose that around half the preexisting open flux in the tail has now been closed, some ~15 GWb, and with the small dayside reconnection rates prevailing, at least during this event as seen in Figure 1, the new open flux created during the interval is small (~1–2 GWb). New closed flux tubes and hot plasma have now rotated from the reservoir in the tail all around the dawn magnetopause to reach the noon sector, such that the dawn region of the former polar cap has now become almost filled with closed flux tubes, precipitating hot plasma, and bright auroras. Discrete and diffuse emissions of lesser intensity continue to be present in the dusk

sector. We propose that this situation is that captured by the HST in Figure 1b. We also suggest that the disturbed auroral distribution presented by *Prangé et al.* [2004] may represent a similar configuration in a tail closure event which was perhaps more impulsive and of lesser intensity.

[24] Figures 10e and 10f then show the situation after ~20 hours, in which the closed flux tubes formed during the event have now rotated back into the nightside sector via Vasyliunas cycle activity at dusk. In the absence of the latter the closed tubes simply rotate directly into the nightside, as shown previously in Figures 3 and 7. We again suppose that tail reconnection is active at modest rates, to which significant but intermittent dayside reconnection is now added. As pointed out previously by *Jackman et al.* [2004], significant open flux production at Saturn's magnetopause also generally occurs during the CIR compression regions, due to the generally elevated values of the compressed IMF. In the present case, Figure 1 suggests the presence of variable dayside reconnection peaking at ~300 kV during the relevant interval. At this stage the compression event has now resulted in the formation of a complete ring of newly injected closed field lines and hot plasma around the planet in the outer magnetosphere, as shown in Figure 10e, such that the region of closed flux has expanded compared with its formerly compressed state. In the ionosphere the newly closed flux forms a spiral around the pole, as shown in Figure 10f, and the dark region of open flux has returned to a more circular form but with a reduced radius compared with its initial value. A more modest bulge persists in the postmidnight sector while tail reconnection is still active, as shown previously in Figure 7, while the band of new closed flux is thinned somewhat in the noon sector and downstream thereof, when magnetopause reconnection is active at appreciable rates, as indicated in section 3.3 in relation to Figure 9. The new open flux rotates into the postnoon and dusk sector, where the open-closed boundary correspondingly begins to expand equatorward. This configuration seems similar to the HST image shown in Figure 1c. We note that according to our discussion the auroral morphology should have evolved appreciably toward that shown in Figure 10f by ~20 hours after the onset of the event (the circulation time in the outer magnetosphere), and it will then remain of similar form while tail reconnection remains active at rates comparable with or larger than the mean dayside rate, as indicated in the discussion of Figure 9a. According to the magnetopause reconnection voltages estimated in Figure 1, the requirement is that the tail reconnection rate should at least exceed ~100 kV. We recall that the HST image shown in Figure 1c corresponds to an interval ~40 hours after the onset of the compression event, from which we infer that conditions then remained as envisaged here in Figures 9a and 10f.

[25] After the initial period of significant reconnection and flux closure in the tail we suppose that the tail reconnection rate drops to smaller values, while the dayside rate remains intermittent but of significant averaged value. The open flux in the tail lobes then starts to expand once more, and with it the size of the dark polar cap in the ionosphere. For example, if the dayside reconnection rate exceeds the nightside rate by an averaged ~100 kV during the final ~2 days of the CIR compression region, as seems plausible from Figure 1 and more generally from the results of *Jackman et al.* [2004], then the net amount of open flux produced will be ~15 GWb, sufficient to reinflate the lobe and polar cap back to its former dimensions. In the HST image shown Figure 1d, ~4.5 days after the onset of compression, the dark polar cap has clearly increased significantly in size, though perhaps not fully to that seen in the image shown in Figure 1a. A more quantitative discussion of these images and their implications for flux changes and reconnection rates, based on the qualitative picture presented here, awaits future analysis. The auroral luminosity in this final image is suggested to be produced by the discrete auroras at the open-closed field line boundary associated with the upward field-aligned currents flowing there, combined with diffuse auroras extending equatorward resulting from precipitation of the hot plasma injected into the outer magnetosphere by the compression event, possibly augmented in the dawn sector in the manner depicted in Figure 9b.

5. Summary and Discussion

[26] The first detailed sequence of images of Saturn's UV auroras were obtained by the HST in January 2004, in coordination with Cassini observations of the upstream interplanetary medium and SKR emissions. These observations show that the auroras and related SKR emissions respond strongly to CIR-related compression regions in the interplanetary medium, the auroras becoming first significantly enhanced and broadened in the dawn sector, before assuming a pronounced spiral form, lasting a few tens of hours after the onset [*Clarke et al.*, 2005; *Crary et al.*, 2005; *Kurth et al.*, 2005]. Possibly related effects have also been reported by *Prangé et al.* [2004], associated in this case with a CME shock tracked to Saturn from the Sun via Earth and Jupiter. We suggest that these effects thus represent the auroral counterparts of the strong solar wind dynamic pressure modulations of SKR emission found previously in Voyager data by *Desch* [1982] and *Desch and Rucker* [1983]. In this paper we provide an interpretative scenario for these observations, based on reconnection dynamics in a rotation-dominated magnetosphere. The picture discussed effectively combines the steady state picture of Saturn's magnetosphere presented previously by *Cowley et al.* [2004a] with the reconnection dynamics discussed by *Cowley and Lockwood* [1992] in the terrestrial context, but with the important effects of planetary rotation at Saturn now included. These concepts are used to discuss the effects of reconnection pulses and of intervals of steady but unbalanced tail and dayside reconnection in Saturn's magnetosphere. It is pointed out that in a rotation-dominated magnetosphere the latter scenario naturally results in the formation of spirals of new open or new closed flux around the rotation axis as the open-closed field line boundary expands or contracts. The sense of the spiral formed by net flux closure is same as that uniquely observed in Saturn auroral images [*Gérard et al.*, 2004; *Clarke et al.*, 2005]. In the simple picture suggested here, therefore, auroral spirals are formed by hot plasma precipitation on newly closed flux tubes and should be observed when the tail reconnection rate exceeds the dayside rate, such that the region of open

flux contracts with time. When the dayside rate exceeds the tail rate, however, such that the open flux region expands with time, the tail-produced spiral will be truncated in the noon sector by dayside reconnection. The aurora will then be enhanced at dawn, though emissions associated with the cusp, open-closed field line boundary, and outer magnetosphere may continue into the dusk sector. These simple pictures assume that the duration of the reconnection intervals exceeds the subcorotational period of outer magnetosphere or polar cap field lines, taken to be roughly ~20 and ~30 hours, respectively. However, the usual fluctuations of the north-south IMF component on shorter timescales implies that this will rarely be satisfied for dayside reconnection, such that an auroral spiral may be formed on closed field lines whenever significant tail reconnection is active, though dayside reconnection may result in significant structuring in the postnoon sector.

[27] Within this picture we then propose that the features observed in the HST auroral data shown in Figure 1 [*Clarke et al.*, 2005], and in related SKR data [*Kurth et al.*, 2005], are produced by the onset of a several-hour interval of rapid reconnection in Saturn's tail, triggered by the sudden magnetospheric compression produced by the forward shock of a CIR compression region in the interplanetary medium. In the several hours following the onset of compression (which overall lasts typically a few days), a significant fraction (around a half) of the open flux in Saturn's tail lobes becomes closed, implying reconnection rates of, e.g., ~500 kV over ~10 hours (or higher values over proportionately shorter intervals). Similar shock-induced major flux closure events have also been reported at Earth on a number of occasions [e.g., *Petrinec and Russell*, 1996; *Sigwarth et al.*, 2000; *Chua et al.*, 2001; *Boudouridis et al.*, 2003, 2004; *Milan et al.*, 2004; *Meurant et al.*, 2004], but, as discussed further below, they may occur more often and more routinely at Saturn, due to the more CIR-evolved nature of the interplanetary medium at these distances and the longer timescales of substorm-related dynamics [*Jackman et al.*, 2004]. The onset of rapid reconnection in the tail initially produces a bulge of newly closed field lines and hot plasma precipitation in the previously dark polar cap region on the nightside, possibly favoring the postmidnight sector. Over subsequent hours these flux tubes will then subcorotate around the magnetopause boundary via dawn, reaching the dayside sector after ~10 hours and forming a complete spiral around the pole after ~20 hours, following which the pattern remains of similar form until the tail reconnection rate declines. The corollary in the magnetosphere is the injection of hot plasma on newly closed flux tubes from the tail around the magnetopause boundary, initially into the dawn sector and later at increasing local times. The flux transport from the tail causes the closed field line region to expand outwards once more, compared with its initially compressed state. We note that the signatures of these phenomena should be apparent in in situ Cassini field and plasma data should a compression event occur when the spacecraft is traversing the outer region of Saturn's magnetosphere, particularly in the postmidnight and dawn sector.

[28] After 1–2 days, however, we propose that the tail reconnection rate drops to smaller values, less than ~100 kV. This effect may be controlled by the concurrent behavior of the dynamic pressure of the interplanetary medium during the event. Since averaged dayside reconnection rates in the high-field intervals of CIR compression regions generally exceed such values [*Jackman et al.*, 2004], the open flux in the system then starts to increase once more, and with it the size of the dark polar cap. We then expect the auroras to revert to a more normal "auroral oval" configuration, possibly with continuing intermittent signatures of reconnection in the dayside cusp (Bunce et al., submitted manuscript, 2004). Typically, the amount of flux which is opened in the last ~2 days of a 4 day CIR compression region is sufficient to reinflate the tail lobe and polar cap back to their former size prior to the compression, as the solar wind dynamic pressure declines. The magnetosphere is then "primed" for the next compression event which may typically occur ~8 days later, though it is possible that significant open field inflation and internally generated tail dynamics may occur in the interval between [*Jackman et al.*, 2004].

[29] Overall, it will be seen that the underlying physics of Saturn's auroral disturbances suggested here, and related effects in the outer magnetosphere, are fundamentally similar to those at Earth, involving open flux transport to and from the tail via the Dungey cycle. However, the auroral morphology to which these processes give rise is strongly influenced by the rapid planetary rotation at Saturn, as described above, while the way in which auroral and other (e.g., SKR) disturbances relate to the interplanetary medium is altered by the differing timescales that apply. At Earth, intervals of southward IMF which inflate the polar cap and tail with open flux often last for tens of minutes to an hour or two, sufficient to bring the tail to instability at the end of substorm "growth phases" which typically last 30–40 min. Consequently, a strong correlation is found in this case between auroral and related disturbances and southward IMF. In addition, the tens of minutes to few-hour timescales of substorms, relative to the few-day typical timescales between interplanetary shocks, shows why shock-induced events will be relatively rare in this case, such that most open flux closure events (specifically substorms) are not triggered by shocks. When shocks do occur, the auroral response is found to depend strongly on the concurrent direction of the IMF, with major "closure" events occurring during intervals of southward directed IMF when the existing auroral oval is relatively expanded, an effect known as "preconditioning" [e.g., *Boudouridis et al.*, 2003, 2004; *Meurant et al.*, 2004]. At Saturn, however, the typical timescales for variations of the north-south component of the IMF are similar to Earth, tens of minutes to a few hours, while the timescale required to bring the tail to instability is much longer, typically many days, as recently discussed by *Jackman et al.* [2004]. In this case it is obvious that a similar correlation of auroral and related disturbances with intervals of northward IMF will not be apparent. In addition, because the expected several-day timescale for substorms at Saturn is comparable to the intervals between interplanetary shocks gen-

erated by recurrent CIRs and CMEs, the probability that an open flux closure event will be initiated in a partly inflated tail by a shock-related magnetospheric compression, rather than a substorm being initiated by an internal instability or external trigger unrelated to shocks [e.g., *Lyons et al.*, 1997], will be greatly enhanced. The response to such shocks will undoubtedly be influenced by magnetospheric preconditioning, as at Earth, but that will now depend upon the past history of the system and interplanetary medium over several previous days, rather than simply on the near-concurrent state of the IMF as at Earth. In the case discussed in this paper, for example, a slow and intermittent accumulation of open flux is expected (on the basis of equation (1)) to have taken place in the several-day rarefaction interval prior to the compression, which will have contributed to the relatively expanded state of the auroral oval observed prior to the event. Overall, we conclude that a significant fraction of open flux closure events at Saturn may be compression-induced, possibly the majority, thus leading to the observed strong correlation between auroral and related disturbances and the dynamic pressure of the solar wind. We may not conclude directly from such a correlation, however, that the underlying physics of the magnetospheric interaction with the interplanetary medium is necessarily of a fundamentally differing character.

[30] **Acknowledgments.** Work at Leicester was supported by PPARC grant PPA/G/O/2003/00013. SWHC was supported by PPARC Senior Fellowship PPA/N/S/2000/00197, and EJB was supported by PPARC Post-Doctoral Fellowship PPA/P/S/2002/00168. J-CG and DG were supported by the Belgian National Fund for Scientific Research (FNRS), and their work was partly funded by the PRODEX program of the European Space Agency (ESA). We thank F.J. Crary and the Cassini CAPS instrument team for use of the solar wind velocity data employed to generate the voltage values shown in Figure 1. CAPS is supported by a contract with NASA/JPL. This work is based on observations with the NASA/ESA Hubble Space Telescope, obtained at the Space Telescope Science Institute, which is operated by the AURA, Inc. for NASA.

[31] Arthur Richmond thanks Athanasios Boudouridis and Michael D. Desch for their assistance in evaluating this paper.

References

Behannon, K. W., R. P. Lepping, and N. F. Ness (1983), Structure and dynamics of Saturn's outer magnetosphere and boundary regions, *J. Geophys. Res.*, *88*, 8791.

Boudouridis, A., E. Zesta, L. R. Lyons, P. C. Anderson, and D. Lummerzheim (2003), Effect of solar wind pressure pulses on the size and strength of the auroral oval, *J. Geophys. Res.*, *108*(A4), 8012, doi:10.1029/2002JA009373.

Boudouridis, A., E. Zesta, L. R. Lyons, P. C. Anderson, and D. Lummerzheim (2004), Magnetospheric reconnection driven by solar wind pressure fronts, *Ann. Geophys.*, *22*, 1367.

Chua, D., G. Parks, M. Brittnacher, W. Peria, G. Germany, J. Spann, and C. Carlson (2001), Energy characteristics of auroral electron precipitation: A comparison of substorms and pressure pulse related auroral activity, *J. Geophys. Res.*, *106*, 5945.

Clarke, J. T., et al. (2005), The nature of Saturn's auroras, *Nature*, in press.

Cowley, S. W. H., and E. J. Bunce (2003b), Modulation of Jupiter's main auroral oval emissions by solar wind-induced expansions and compressions of the magnetosphere, *Planet. Space Sci.*, *51*, 57.

Cowley, S. W. H., and M. Lockwood (1992), Excitation and decay of solar wind-driven flows in the magnetosphere-ionosphere system, *Ann. Geophys.*, *10*, 103.

Cowley, S. W. H., M. P. Freeman, M. Lockwood, and M. F. Smith (1991), The ionospheric signature of flux transfer events, in *Cluster: Dayside Polar Cusp*, *Eur. Space Agency Spec. Publ.*, *ESA SP-330*, 105.

Cowley, S. W. H., E. J. Bunce, and R. Prangé (2004a), Saturn's polar ionospheric flows and their relation to the main auroral oval, *Ann. Geophys.*, *22*, 1379.

Cowley, S. W. H., E. J. Bunce, and J. M. O'Rourke (2004b), A simple quantitative model of plasma flows and currents in Saturn's polar ionosphere, *J. Geophys. Res.*, *109*, A05212, doi:10.1029/2003JA010375.

Crary, F. J., et al. (2005), Solar wind control of Saturn's auroras, *Nature*, in press.

Desch, M. D. (1982), Evidence for solar wind control of Saturn radio emission, *J. Geophys. Res.*, *87*, 4549.

Desch, M. D., and H. O. Rucker (1983), The relationship between Saturn kilometric radiation and the solar wind, *J. Geophys. Res.*, *88*, 8999.

Dungey, J. W. (1961), Interplanetary field and the auroral zones, *Phys. Rev. Lett.*, *6*, 47.

Galopeau, P. H. M., P. Zarka, and D. LeQuéau (1995), Source location of Saturn's kilometric radiation: The Kelvin-Helmholtz instability hypothesis, *J. Geophys. Res.*, *100*, 26,397.

Gérard, J.-C., V. Dols, D. Grodent, J. H. Waite, G. R. Gladstone, and R. Prangé (1995), Simultaneous observations of the Saturnian aurora and polar haze with the HST/FOC, *Geophys. Res. Lett.*, *22*, 2685.

Gérard, J.-C., D. Grodent, J. Gustin, A. Saglam, J. T. Clarke, and J. T. Trauger (2004), Characteristics of Saturn's FUV aurora observed with the Space Telescope Imaging Spectrograph, *J. Geophys. Res.*, *109*, A09207, doi:10.1029/2004JA010513.

Gosling, J. T., and V. J. Pizzo (1999), Formation and evolution of corotating interaction regions and their three dimensional structure, *Space Sci. Rev.*, *89*, 21.

Isbell, J., A. J. Dessler, and J. H. Waite Jr. (1984), Magnetospheric energization by interaction between planetary spin and the solar wind, *J. Geophys. Res.*, *89*, 10,716.

Jackman, C. M., N. Achilleos, E. J. Bunce, S. W. H. Cowley, M. K. Dougherty, G. H. Jones, S. E. Milan, and E. J. Smith (2004), Interplanetary magnetic field at ~9 AU during the declining phase of the solar cycle and its implications for Saturn's magnetospheric dynamics, *J. Geophys. Res.*, *109*, A11203, doi:10.1029/2004JA010614.

Kurth, W. S., et al. (2005), Ultraviolet aurora and kilometric radio emissions: Two views of Saturn's auroras, *Nature*, in press.

Lecacheux, A., and F. Genova (1983), Source location of Saturn kilometric radio emission, *J. Geophys. Res.*, *88*, 8993.

Lyons, L. R., G. T. Blanchard, J. C. Samson, R. P. Lepping, T. Yamamoto, and T. Moretto (1997), Coordinated observations demonstrating substorm triggering, *J. Geophys. Res.*, *102*, 27,039.

Meurant, M., J.-C. Gérard, C. Blockx, B. Hubert, and V. Coumans (2004), Propagation of electron and proton shock-induced aurora and the role of the interplanetary magnetic field and solar wind, *J. Geophys. Res.*, *109*, A10210, doi:10.1029/2004JA010453.

Milan, S. E., S. W. H. Cowley, M. Lester, D. M. Wright, J. A. Slavin, M. Fillingim, C. W. Carlson, and H. J. Singer (2004), Response of the magnetotail to changes in the open flux content of the magnetosphere, *J. Geophys. Res.*, *109*, A04220, doi:10.1029/2003JA010350.

Milan, S. E., E. J. Bunce, S. W. H. Cowley, and C. M. Jackman (2005), Implications of rapid planetary rotation for the Dungey magnetotail of Saturn, *J. Geophys. Res.*, *110*, doi:10.1029/2004JA010716, in press.

Ness, N. F., M. H. Acuña, R. P. Lepping, J. E. P. Connerney, K. W. Behannon, L. F. Burlaga, and F. M. Neubauer (1981), Magnetic field studies by Voyager 1: Preliminary results at Saturn, *Science*, *212*, 211.

Ness, N. F., M. H. Acuña, K. W. Behannon, L. F. Burlaga, J. E. P. Connerney, R. P. Lepping, and F. Neubauer (1982), Magnetic field studies by Voyager 2: Preliminary results at Saturn, *Science*, *215*, 558.

Petrinec, S. M., and C. T. Russell (1996), Near-Earth magnetotail shape and size as determined from the magnetopause flaring angle, *J. Geophys. Res.*, *101*, 137.

Prangé, R., L. Pallier, K. C. Hansen, R. Howard, A. Vourlidas, R. Courtin, and C. Parkinson (2004), An interplanetary shock traced by planetary auroral storms from the Sun to Saturn, *Nature*, *432*, 78.

Richardson, J. D. (1986), Thermal ions at Saturn: Plasma parameters and implications, *J. Geophys. Res.*, *91*, 1381.

Richardson, J. D. (1995), An extended plasma model for Saturn, *Geophys. Res. Lett.*, *22*, 1177.

Richardson, J. D., and E. C. Sittler Jr. (1990), A plasma density model for Saturn based on Voyager observations, *J. Geophys. Res.*, *95*, 12,019.

Saur, J., B. H. Mauk, A. Kassner, and F. M. Neubauer (2004), A model for the azimuthal plasma velocity in Saturn's magnetosphere, *J. Geophys. Res.*, *109*, A05217, doi:10.1029/2003JA010207.

Sigwarth, J. B., L. A. Frank, and N. J. Fox (2000), The effect of a dynamic pressure pulse in the solar wind on the auroral oval, total open magnetic flux of the polar cap and the auroral ionosphere, paper presented at 33rd COSPAR Scientific Assembly, Comm. on Space Res., Warsaw, Poland.

Sittler, E. C., Jr., K. W. Ogilvie, and J. D. Scudder (1983), Survey of low-energy plasma electrons in Saturn's magnetosphere: Voyagers 1 and 2, *J. Geophys. Res.*, *88*, 8847.

Smith, E. J., L. Davis Jr., D. E. Jones, P. J. Coleman Jr., D. S. Colburn, P. Dyal, and C. P. Sonett (1980), Saturn's magnetosphere and its interaction with the solar wind, *J. Geophys. Res.*, *85*, 5655.

Stallard, T. S., S. Miller, L. M. Trafton, T. R. Geballe, and R. D. Joseph (2004), Ion winds in Saturn's southern auroral/polar region, *Icarus*, *167*, 204.

Trauger, J. T., et al. (1998), Saturn's hydrogen aurora: Wide field and planetary camera 2 imaging from the Hubble Space Telescope, *J. Geophys. Res.*, *103*, 20,237.

Vasyliunas, V. M. (1983), Plasma distribution and flow, in *Physics of the Jovian Magnetosphere*, edited by A. J. Dessler, p. 395, Cambridge Univ. Press, New York.

Vasyliunas, V. M. (1994), Role of the plasma acceleration time in the dynamics of the Jovian magnetosphere, *Geophys. Res. Lett.*, *21*, 401.

S. V. Badman, E. J. Bunce, S. W. H. Cowley, C. M. Jackman, S. E. Milan, and T. K. Yeoman, Department of Physics and Astronomy, University of Leicester, Leicester LE1 7RH, UK. (swhc1@ion.le.ac.uk)

J. T. Clarke, Center for Space Physics, Department of Astronomy, Boston University, 725 Commonwealth Avenue, Boston, MA 02215, USA.

J.-C. Gérard and D. Grodent, Institut d'Astrophysique et de Géophysique, Université de Liège, Allée du 6 Août – Sart Tilman, B-4000 Liège, Belgium.